PULSE-INDUCED CRITICAL SCATTERING AND THE CHARACTERISATION OF POLYMER SAMPLES

H. Galina*, M. Gordon, P. Irvine** and L.A. Kleintjens***

Institute of Polymer Science, University of Essex, Colchester, England.

Abstract - An instrument, developed over the last decade, and now made available, for measuring Pulse-induced Critical Scattering (PICS) intensities, serves a variety of purposes: to explore phase relationships in blends, to aid in refining statistical thermodynamic models for polymer solutions, and to characterise polymer samples. This last aspect is here explored in relation to the high 'tail' of the molecular weight distribution (MWD), which critically affects the slow relaxation to equilibrium of samples in the last stages of manufacture e.g. in die-swell ratios. Polystyrene/cyclohexane solutions are studied and demonstrate the sensitivity of spinodal curves, even greater sensitivity of cloud-point curves, to higher moments of the MWD. Effects due to M_{z+1} are easily observed, which reflect a pattern predicted on mild assumptions from statistical -thermodynamic models. The general philosophy of characterisation is briefly reviewed. Sensitive techniques which explore the region of undisturbed dimensions and balanced interactions are valuable and complementary to GPC.

1. INTRODUCTION

The PICS technique (Ref.1-6) was developed at our Institute of Polymer Science during the 1970's, with much cooperation from Koningsveld and co-workers at the Central Laboratory of the DSM Company in Holland. The Mark III instrument (Fig. 1) is very fully automated and computerised. The instrument and its mode of operation will be described in a forthcoming publication. The basic principles remain those of the Mark II already described (Ref. 3 & 4). The instrument measures intensities of laser light scattered at selected angles (30 and 90°) from ca. 10 mg samples contained in capillary cells during a few seconds following each one of a sequence of periodic thermal steps or 'pulses'. Successive pulses step the sample from a fixed starting temperature in the stable region (Fig. 2), to temperatures which approach (in steps of about 0.01°C) ever more closely to a region of phase separation. By monitoring the light scattering response at 0.01°C intervals, each time just before the sample is sent back to the stable temperature range, much sensitive thermodynamic information is obtained. In particular, so-called spinodals and cloud-point curves (CPC's) are obtained, from which phase diagrams are constructed of spinodal temperatures (T_s) or cloud-point temperatures T_{cl} against concentrations of a polymer in solution (or blends), expressed as weight fraction w or volume fraction ϕ. A typical schematic diagram in Fig. 2 shows the phase diagram near the familiar upper critical solution temperature UCST of a binary system, i.e. a homodisperse polymer in a pure solvent. The PICS instrument is designed to exploit the sensitive scattering behaviour in the metastable region of the phase diagram, between T_s and T_{cl}, where large fluctuations in refractive index occur. The molecular origin of these fluctuations lies, of course, in the concentration fluctuations which are schematized in the panels B and E at the two sides of the diagram. These fluctuations lead to a short-lived metastable equilibrium, followed by nucleation and rapid growth of macroscopic emulsion particles consisting of a separated second phase (panels C,F). The instrument avoids this catastrophe by returning the sample to the safety of the stable temperature zone after a few seconds during which the scattering from fluctuations in metastable equilibrium has been measured repeatedly, analysed, and stored in the computer memory. In the stable temperature zone, fluctuations in the single-phase system are minimal (panels A,D). The scattering intensity from the sample cell in this temperature range is also measured and substracted automatically from the high intensity observed during scattering from

Present address:* Institute of Organic and Polymer Technology, Technical University, 50-370 Wrocław, Poland: ** Department of Chemistry, Stanford University, Stanford, California 94305, U.S.A.: ***Central Laboratory, DSM, Geleen, Netherlands.
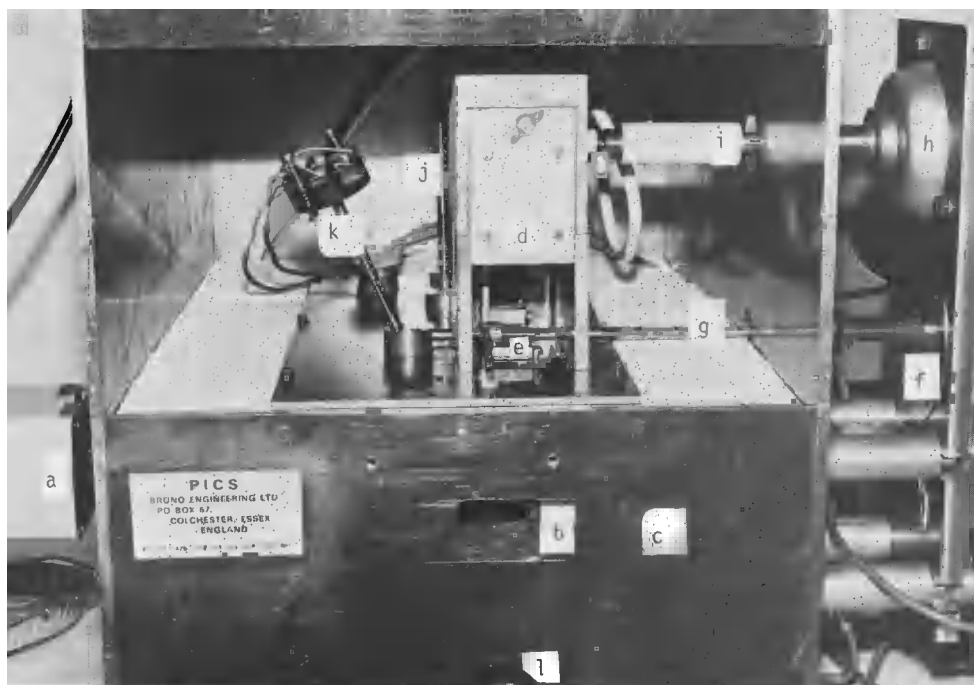
Fig. 1. Central part of the Mark III PICS Instrument. a Helium Neon laser.
b Viewing window aligned with scattering cell immersed in: c oil bath. d Hot
chamber with lid lifted to expose: e one of four cell holders, mounted on carousel,
bearing horizontal capillary scattering cell. f Fast stepping motor for periodic
90° circular permutation of positions of the four cell holders, via: g shaft
of stepping motor. h fan motor for circulating air in hot box, using: i shaft.
j Shaft of bath stirrer. k Pt resistance thermometer. l light-guide entry port.

fluctuations in the metastable temperature range. The reciprocal difference in scattering
intensity at low angle (30°) is then plotted, following Scholte (7). As shown in Fig. 3,
the plots serve to locate T_s as intercept on the temperature axis. Points of extremely high
scattering intensity (close to the T-axis) deviate from the linear plot for theoretically
well understood reasons and are, therefore, rejected by the computer, using objective
statistical criteria. The intercept T_s is located to a precision in the range between 0.02
and 0.1° depending on conditions, particularly depending on how close T_s is to the critical
temperature T_c where measurements are most accurate (-compare Table I later).

2. CRITICAL POINTS

Measurements in this critical region, have a potential yet to be tapped more fully for the
characterisation of polymers, especially as regards their molecular weight distribution
(MWD). The critical point, at which the spinodal curve and CPC touch and share a common
tangent (second-order contact point), is itself very sensitive to polydispersity. It lies
at the maximum (UCST) as shown in Fig. 2, or minimum (LCST), only in strictly homodisperse
polymer solutions in a pure solvent. For polydisperse polymer solutions, the critical
temperature T_c remains a second-order contact point, but is located along the high-
concentration side (Ref. 8) of the extremum (e.g. downwards on the right-hand side in Fig. 2).

Critical points are directly measured only roughly by PICS, in terms of interpolation
to the point of closest approach between spinodal curve and CPC. For reasons to be
discussed elsewhere, the two curves tend to remain separated by an interval ΔT typically
of about 0.1° at their closest approach, instead of showing $\Delta T=0$ at T_c, when direct PICS
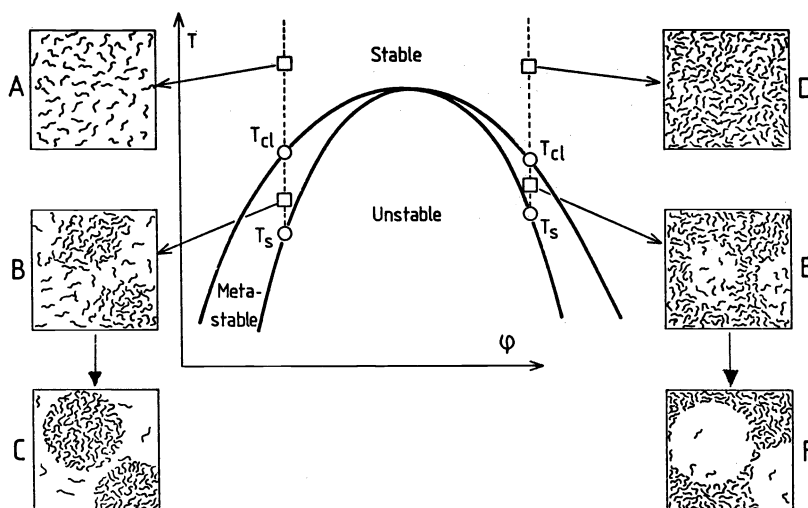
Fig. 2. Typical phase diagram of temperature versus volume fraction. T_{cl} cloud points, T_s spinodal points. Each PICS 'pulse' takes a sample cell from a position in the stable domain (upper square) to a position near the spinodal locus, typically in the metastable domain (lower square), as illustrated for dilute solutions on the left, and for concentrated solutions on the right. The transfer is effected by the stepping motor (Fig. 1), which turns the carousel through 90° to carry the cell from the hot box (Fig. 1, c and d) into the oil bath (Fig. 1, a) in line with the laser beam.

measurements of both curves are plotted. This small discrepancy can safely remain uncorrected for the present purpose; it is perceptible by inspection of columns 3 and 4 in Table I presented later. The exact reference method for locating critical points, viz. the phase volume ratio method of Koningsveld and Steverman (9), agrees well (Ref. 10) with the point of closest approach of spinodal and CPC. The phase volume method has recently been speeded up about ten-fold by exploiting a new instrument, the centrifugal homogeniser (Ref. 11). This device is also valuable for homogenising the contents of PICS light scattering cells, as it solves the problem of how to produce equilibrium single-phase samples by homogenising a few mg of several viscous phases confined in a capillary under high vacuum, while controlling the time-temperature schedule during the course of this homogenisation process.

Leaving aside the use of critical point measurements, this paper is confined to the potential of spinodals and CPC's for polymer characterisation.

3. THE CONCEPT OF MOMENT-EXPANSION AND r-EQUIVALENCE OF MWD's

To rationalise the role of phase equilibrium curves in characterisation we must consider the moments of the MWD of a polymer. The first moment M_1 will be taken as the weight average M_w. The ratio M_2/M_1 of the second to the first moment is then the z-average M_z, etc. We shall usually cite molecular masses in kg mol^{-1} rather than weights. Two MWD's are called r-equivalent (Ref. 3) if they share identical values of the first r moments; they may differ in their higher moments. Computer algorithms (Ref. 12 & 13) can calculate the composition of mixtures which are r-equivalent (for r=1,2,...) to a distribution given in mathematical form, and which mixtures will contain r/2 monodisperse fractions if r is even, and (r+1)/2 such fractions otherwise. Such a computation by Irvine (12) is illustrated in Fig. 4 for the specific Flory weight-fraction distribution

$$w_m = 10^{-10} \, Me^{-M/100,000} \tag{1}$$

with 2-8 fractions. The figure shows how the increasing number of fractions progressively
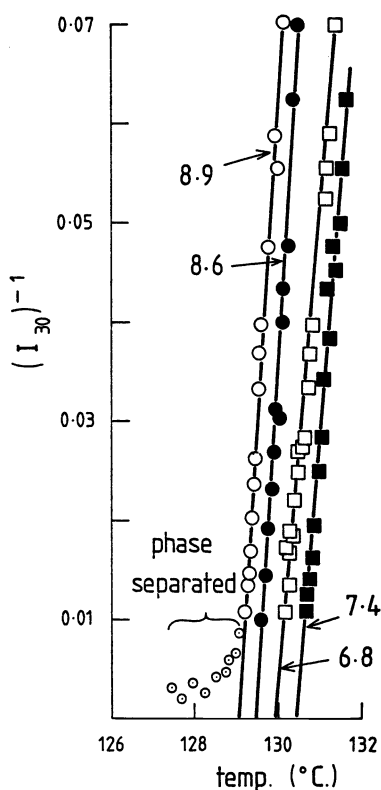
Fig. 3. Typical experimental Debye-Scholte plot for system polyethylene/diphenyl ether at four weight percent concentrations shown (Ref. 16). Linear polyethylene, M=160 kg mol^{-1}. Reciprocal light scattering intensity is plotted against temperature, to obtain the spinodal by short extrapolation to the T-axis. Points on each line were measured in descending order. Total measuring time typically ca. 30 min. for the four cells. The data are stored automatically, and subsequently computer-plotted.

simulates more closely the course of the continuous distribution curve. In a very practical sense, an r-equivalent mixture simulates a distribution in an optimal way for matching physical properties. The more sensitive the property is to the high tail of the MWD, the larger r should be taken. When the distribution to be matched is not given in mathematical form (as in eq. 1), but as an experimental curve e.g. by GPC, it can first be matched mathematically, e.g. by a linear combination of Schulz-Zimm distributions, using well-known curve-matching programmes. The mathematical form thus obtained can be converted to an r-equivalent distribution of a few sharp fractions using available programmes (Ref. 13). While for continuous distributions, spinodals, and particularly CPC's, are beyond our power to compute, except for unrealistically simple ΔG-functions, excellent fittings of models are achieved in terms of r-equivalent mixtures for r=3 in many cases (Ref.3 & 6). The rest of this paper is largely concerned with demonstrating this concept as an aid in characterisation. As a simple extension of the concept, series of different mixtures of available "homodisperse" fractions can be computed. The moments M_1 to M_3 of such fractions being known within

reasonable limits (see later, Table II), the mixtures have (pre-selected) moments M_1-M_3 whose values are usually substantially more reliable (later, Table III) than those of available samples obeying a 'continuous' MWD.

4. MOMENT EXPANSION OF THE CLOUD-POINT CURVE

As an application of r-equivalence, we show in Fig. 5 calculation of the CPC, in terms of a moment expansion, for a Flory (most probable) distribution based on a rather complex theoretical free energy of mixing function, ΔG_{mix}, given by eq. 7 in Ref. 6. This is a 'pre-averaged' version, extending to polydisperse polymer solutions, the model of Koningsveld

et al (Ref. 14) for homodisperse ones. Their 'bridging' model (cf. Ref. 3) tries to
link up smoothly the thermodynamic behaviour of dilute polymer solutions, where the coils
are isolated, through the difficult semi-dilute range, with the more concentrated range of
fully over-lapping coils modelled by the Flory-Huggins theory. The pre-averaged model fitted
literature values of critical points of solutions of polystyrene (PS) in cyclohexane (CH)
often within experimental error (Ref. 6). The model has been both simplified and improved
by further refinement (eq. 10 of Ref. 6) but the parameters for predicting CPC's in Fig. 5,
and the ΔG_{mix} used for that purpose, dispensed with this simplification. The calculation
of a CPC for such a realistic model ΔG function, when more than a few different chain-
lengths are present, is at present impossible. Figure 5 shows (Ref. 12), however, that a
moment-expansion, which appears to converge well, can be carried out in terms of r-
equivalent mixtures up to r=10. Experimentally, discrimination between curves F8 (four
sharp fractions) and 10 (five sharp fractions) would be possible at best for concentrations
ϕ<0.03, while above this limit the curves are practically coincident. No experimental
technique can check whether the distribution in a polymer sample has moments above M_{10}
(or averages beyond M_{z+8}) which actually obey the Flory distribution law, and, in any case,
curve F10 must be practically indistinguishable from the limiting curve for the experiment-
ally significant concentration range.

5. TRUNCATION OF MOMENT-EXPANSIONS

The pattern of the family of CPC's in Fig. 5, rather than the precise course of the curves,
is highly significant for efforts to characterise polymers. The critical points of the
computed CPC's lie beyond the concentration of ϕ = 0.07 to which Fig. 5 extends on the right.
There is a considerable trend towards convergence of the curves as they approach their
critical points, and conversely the curves fan out at high dilution; this is the character-
istic of special interest. Theory shows it to be a pattern quite generally expected irres-
pective of the specific form of the free energy of mixing adopted for modelling a polymer
solution. The pattern signifies that the effects of higher moments of the MWD, i.e. of the
tail of high molecular weights, on the CPC becomes systematically larger as ϕ decreases.
A similar fanning out is predicted theoretically, and generally, for increasing ϕ beyond ϕ_c.

The convergence of spinodals at ϕ_c is regulated by truncation theorems (Ref.3 & 15), which
lay down truncation limits for an extremely wide class of ΔG_{mix}-functions which generalise
the Flory-Huggins model, i.e. limits beyond which higher moments leave the spinodal, or the
critical point, strictly invariant towards changes in higher moments. These theorems have
been rigorously proved from thermodynamics (Ref. 15). Applied to the specific form of the
pre-averaged bridging model (i.e. the ΔG_{mix} of eq. 7, (Ref. 6)), used in computing the
family of CPC's r-equivalent to a Flory distribution, the following conclusions are exact:
the curves 6, 8, and 10 must converge at their common critical point (not shown) without
intersection, and then separate again when $\phi \gtrsim \phi_c$. This follows, because a) the critical
points ϕ_c of this ΔG_{mix}-function are exactly fixed by the first five moments of the MWD,
and because spinodals and CPC's have second-order contact at ϕ_c. Spinodals for this ΔG_{mix}
are, moreover, fully determined throughout their course by the first three moments (M_1 to M_3).

While CPC's are not subject to truncation, i.e. in principle all moments affect their course,
the dependence on moments higher than the truncation limit for spinodals must dwindle to
insignificance near ϕ_c, where CPC and spinodal curve approach coincidence. We turn to
comparing these patterns of behaviour with experiments on the best-known system.

6. EXPERIMENTAL: SPINODALS AND CPC's OF MIXTURES OF SHARP FRACTIONS IN SOLUTION

In Fig.6 & 7, experimental CPC's and spinodals respectively are given for six polystyrene
samples in cyclohexane, for which experimental points are tabulated in Table I. These
samples, labelled A-F, consisted of blends made from two to four (out of six available)
sharp fractions as detailed in Table II. Five of the six sharp fractions (Pressure
Chemicals) were characterised in the DSM laboratories in the Netherlands by GPC for
M_n, M_w and M_z; by light-scattering for M_w; by osmotic pressure for M_n; and by ultracentrifuge
for M_w and M_z. The sixth sharp fraction (PS2) was assigned values quoted by the manufact-
urers and by PICS spinodals. The accepted values of the M_n, M_w and M_z, and their standard
deviations, are summarised in Table III. Values of the computed molecular weight averages
for the six blends A-F are given in Table IV. Table III also includes estimates of M_{z+1}
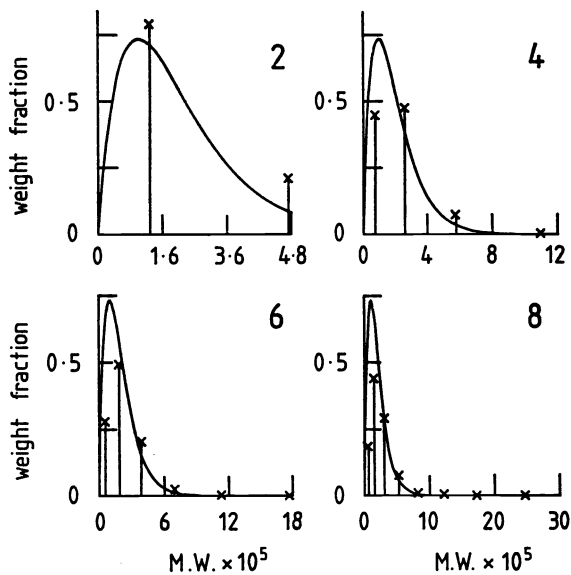
Fig. 4. Uniquely determined normalized sets of 2,4,6 or 8 homodisperse fractions, which are r-equivalent mixtures, r=3,7,11 and 15 respectively, to the Flory weight-fraction distribution (eq.1) curve shown.
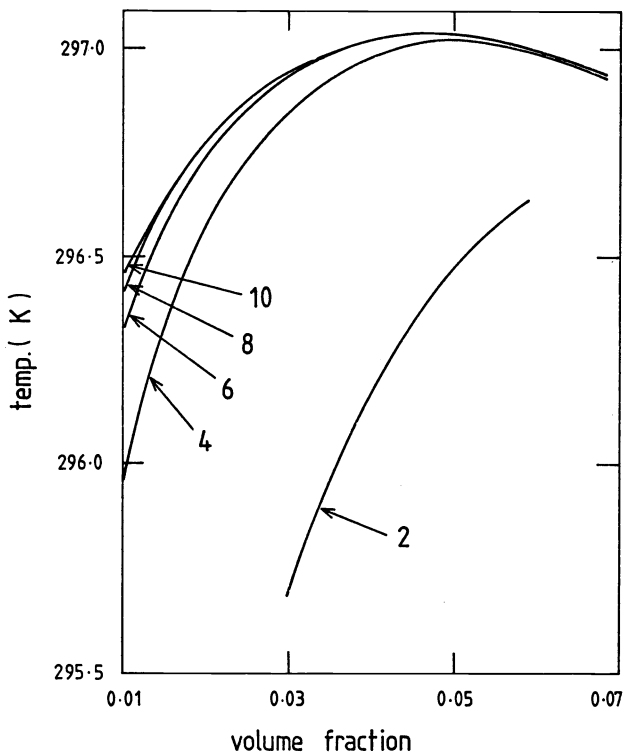
Fig. 5. Family of cloud-point curves calculated for mixtures r-equivalent to a Flory distribution (eq.1), of polystyrene in cyclohexane, using eq.7 of Ref. 6 for ΔG-function; r=2,4,6,8,10 as shown. Note fanning-out towards low volume fraction end, and convergence of curves as r increases.
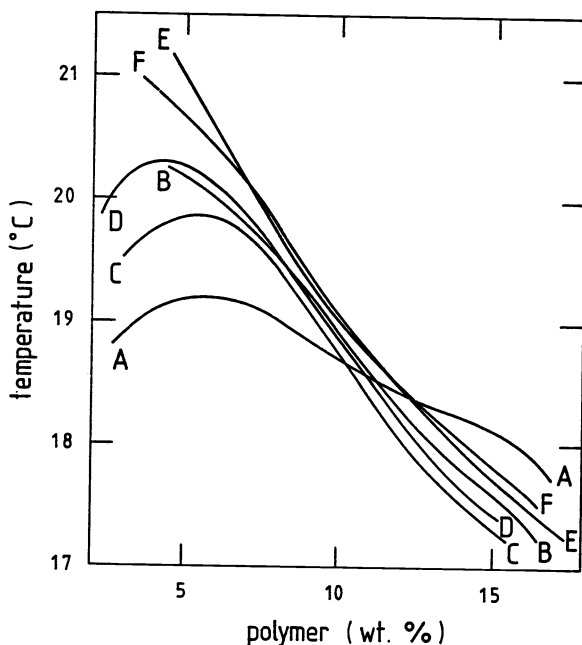
Fig. 6. Smoothed cloud-point curves (Table I), measured by PICS with the 'seeded-emulsion' technique (Ref. 3), for six blends (Table II,IV) of polystyrene in cyclohexane

given in the form of an upper (u) limit M_{z+1}^u, calculated from the assumed equation

$M_{z+1}/M_z = M_z/M_w$. Thus M_{z+1} would be correctly calculated as $M_{z+1} = M_{z+1}^u$ for a (very broad)

log-normal type of distribution, but $M_{z+1} < M_{z+1}^u$ for a (rather broad) Flory distribution.

We may therefore be confident that $M_{z+1} < M_{z+1}^u$ also for our mixtures of sharp fractions.

In Table IV, the upper bounds M_{z+1}^u of the blends were computed from their compositions

(Table II), using M_{z+1}^u values for each component fraction. The lower bounds M_{z+1}^ℓ were found

by using M_z values as lower bounds in place of M_{z+1} for each component fraction. Since

blending of fractions can be done with the accuracy limited essentially only by that of the

analytical balance, we may be fairly confident that the true M_{z+1} values are equal to the

mean between M_{z+1}^ℓ and M_{z+1}^u to within 15 per cent, so allowing also for the possible errors

(Table III) in M_z and M_w which enter the calculation.

7.1 THE VALUE OF SPINODAL AND CLOUD-POINT MEASUREMENTS

i) Spinodals

Cloud-points can be measured over a wider range of concentrations and somewhat more precisely than spinodals. Nevertheless, spinodal measurements have substantial value. In a systematic attack on problems of characterisation, or in refining thermodynamic models of polymer solutions, measurements of spinodals should precede cloud-points. Cloud-points are much more sensitive, e.g. to the MWD, and a less sensitive variable has preference for the purposes of initial orientation. Of course, near the critical point, the CPC has second-order contact with the spinodal, i.e. the two measurements should agree within experimental error in some range about this point. But how fast they diverge from one another as concentrations further from the critical are explored, depends on averages above M_z, to which

CPC's but not spinodals are sensitive. This theoretically predicted differential sensitivity is well borne out by a comparison between the spinodals in Fig. 7 and the corresponding CPC's in Fig. 6. Thus the spinodals of samples B-F remain identical (within the calibration errors of the molecular weights of their constituent fractions) over the whole experiment-ally accessible range in Fig. 7, which has a much expanded temperature scale. These samples were prepared so as to agree in M_w and M_z, though not in higher averages. The spinodal
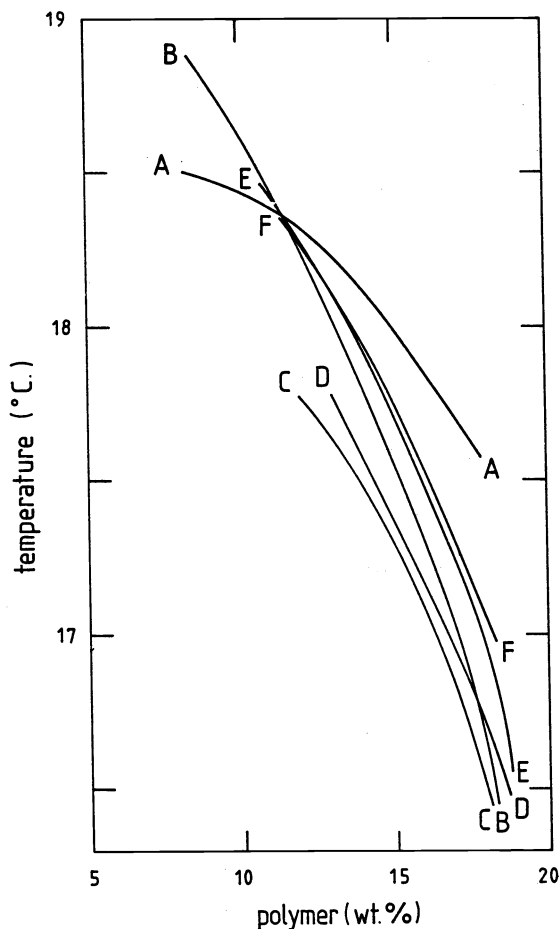
Fig. 7. Smoothed spinodals (Table I), measured by PICS, of the same six blends as in Fig. 6.

measurements thus provide a tool for focussing on M_w and M_z to the safe exclusion of effects due to higher averages and so of effects due to small amounts of high molecular weight tails, e.g. 0.4 per cent of PS6 (M=692) in sample E (Table II & III). Spinodals discriminate between effects of M_w and M_z as sensitively as do CTC's since small differences in M_z are reflected in substantial changes in the slope (common to both kind of curves) dT/dw at the critical point. This is seen for sample A whose spinodal and CPC stand apart from those of the other samples, because A features a value of M_z estimated to be 28% lower (Table IV).

The critical concentrations of all the samples lie around w=0.12 - 0.14, and the inter-section of both phase loci for sample A with those of the samples B-F occurs near this critical concentration range. In Fig. 8, the sensitivity of spinodals to M_w and M_z is seen over a wider (though still modest) range. The circles and triangles show that the spinodal of sharp fractions is displaced by nearly 3° for a change in M_w from 120 to 200. In this range, differences in M_w of sharp fractions can be readily measured by PICS to 1 kg mol^{-1} by locating their spinodals. Comparing the circles and squares shows the effect of doubling M_z for fixed M_w, leading to a tilting (steepening) in the plot of T_s against w. This tilt-ing is predicted quantitatively (Ref. 6) and characteristic of the fractionation effects which dominate the entropy of mixing of polydisperse solutions. The extension of the measurable range of the polydisperse sample (squares) towards higher concentrations is connected with the displacement of the critical point (not shown) in the same direction, when compared to the nearly homodisperse polymer (circles) of equal M_w. While spinodals are insensitive to M_n, except at very low M_n and M_w, Fig. 7 shows the valuable sensitivity of PICS measurements to changes in M_w and M_z. A final point in favour of spinodal
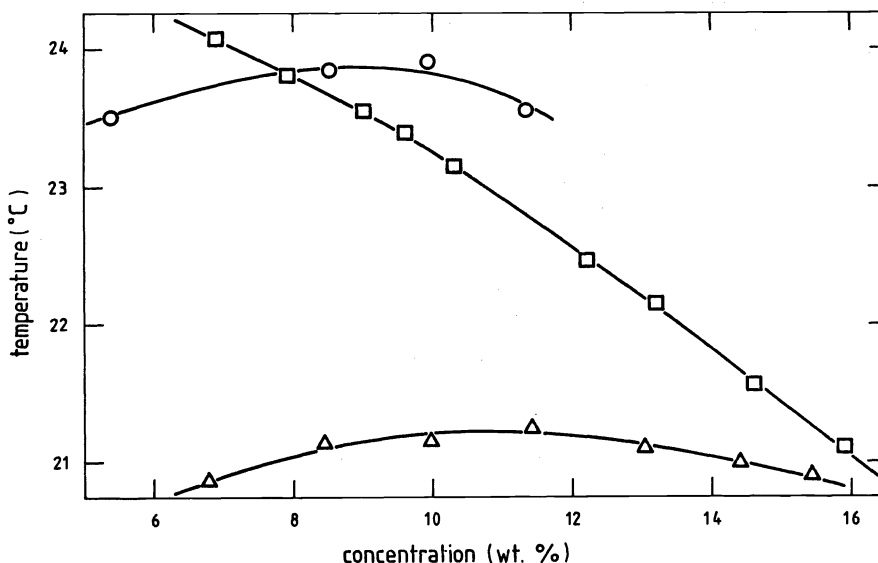
Fig. 8. Typical flat spinodal curves for PS in CH for two sharp fractions and one typical 'tilted' spinodal curve for a polydisperse blend. O M_n 193, M_w 200,($M_z \sim M_w$); △ M_n 111, M_w 120,($M_z \sim M_w$); ▢ M_n 49, M_w 200, M_z 450. (Ref. 17)

measurements is the fact that they can be calculated from theoretical thermodynamic models much more simply than CPC's, a feature that gives confidence in their interpretation. This use of spinodals has been demonstrated (Ref. 6) by fitting hundreds of measurements on the same system PS/CH, covering a forty-fold molecular weight range and about a range of 19^0, using the ΔG_{mix}-function of a refined and simplified model. The sensitivity of spinodals to branching of polymers was explored elsewhere (Ref. 16).

ii) Cloud-point curves

The great value of CPC's when used in conjunction with spinodals, is their progressively and systematically increasing sensitivity to higher averages beyond M_z as we pass to high or (especially) to low concentrations away from the critical. All the CPC's in Fig. 6 pass close to the point w = 0.12, T = 18.5^0, say, a feature attributable to the constancy of M_w and M_z. As we move towards lower concentrations, the curves of samples B-F remain close together over a substantial concentration range, a feature of reflecting constancy of M_z.

However, as predicted by theory (see §5), the CPC's eventually fan out, strongly below w = 0.07 and weakly above 0.15. The expectation that this fanning out would systematically reflect variations in M_{z+1} is borne out rather well except for sample B (whose 'misbehaviour' is slightly reflected in the spinodal curve also, Fig. 7). To put this 'misbehaviour' into perspective, we remark that, by using the CPC's of samples C,D,E and F as calibration marks for estimating M_{z+1} of B by interpolation, we would estimate a value around 220, instead of the value 186±28 deduced in Table III from the absolute calibration of lower moments of the two fractions from which sample B was mixed. Attempts to measure M_{z+1} of sample B absolutely, presumably by ultracentrifuge, would hardly do better!

7.2 THE WAY FORWARD IN THE CHARACTERISATION OF POLYMERS

There are serious gaps in the armoury of characterisation equipment for polymer technology, where fabrication procedures may show up mysterious differences between technical products of polymer manufacture, which fail to be discriminated by available fundamental character-isation instruments. In respect of such sensitive properties, technical samples are in practice usually graded by non-fundamental test procedures (e.g. melt index), which simulate production processes. These properties are likely to be sensitive not merely to the MWD, and especially its higher moments, but also to branching, tacticity and other variations in microstructure. These aspects, though usually beyond sufficiently quantitative fundamental characterisation, need to be tackled by systematic studies with a choice of appropriate tools.

TABLE I. Spinodal and cloud point measurements

Mixtures	Wt. % Polymer,w	T_s (°C)	T_{cl} (°C)	Mixtures	Wt. % Polymer,w	T_s (°C)	T_{cl} (°C)
1	3.38		18.82	2	4.96		20.19
	4.46		19.20		5.21		20.11 (.1)
	5.38		19.11 (.1)		8.37	18.80(.06)	19.52
	7.06		19.19		8.84	18.87(.09)	19.36
	7.50		19.12		10.52		18.83(.03)
	8.86		18.80		11.77	18.41(.02)	18.43(.02)
	9.36		18.90(.02)		12.80	17.87(.03)	18.13(.02)
	10.16	18.42(.05)	18.71(.03)		14.02	17.65(.05)	17.81(.02)
	11.38	18.38(.04)	18.59(.02)		14.25	17.61(.04)	17.88(.03)
	12.30	18.38(.04)	18.46(.03)		14.65	17.63(.04)	17.73(.03)
	13.91	18.06(.04)	18.22(.02)		16.47	17.19(.08)	17.29(.03)
	15.12	17.98(.03)	18.16(.02)		18.01	16.57(.02)	16.66(.03)
	15.77	17.96(.02)	18.09(.02)	4	2.68		19.97
	16.98	17.70(.04)	17.78(.03)		2.40		19.93
	18.23	-	17.76(.02)		2.83		20.20
	19.73	16.99(.07)	17.39(.03)		4.25		20.33 (.1)
3	3.57		19.70		5.04		20.24
	5.47		19.86 (.1)		6.37		20.05
	6.57		19.84		7.70		19.62
	8.61		19.21		9.20		19.14
	10.65		18.63(.04)		10.94		18.71(.04)
	12.78		17.81(.03)		12.80	17.75(.06)	18.03(.02)
	12.07	17.75(.03)	-		13.86	17.65(.07)	17.74(.02)
	14.48	17.37(.04)	17.52(.04)		14.78	17.44(.03)	17.54(.02)
	15.51	17.18(.03)	17.29(.02)		16.01	17.11(.07)	17.42(.02)
	17.56	16.61(.02)	16.70(.02)		18.58	16.48(.04)	16.62(.03)
	18.14	16.45(.02)	16.51(.02)	6	4.66		21.06
5	3.80		21.00		5.36		20.95
	4.73		20.71		6.81		20.26 (.1)
	5.38		20.50 (.1)		7.39		19.95
	5.84		20.65		9.41		19.26
	6.99		20.24		11.71	18.28(.05)	18.53(.04)
	7.44		19.99		12.48	18.21(.06)	18.44(.03)
	9.92		19.14(.04)		13.61	18.07(.05)	18.11(.02)
	11.53	18.37(.03)	18.67(.03)		14.59	17.78(.06)	17.94(.03)
	13.37	18.06(.03)	18.16(.02)		15.28	17.62(.05)	17.82(.03)
	15.26	17.60(.06)	17.71(.03)		16.69	17.32(.04)	17.55(.03)
	15.62	17.51(.02)	17.67(.03)		18.25	16.99(.06)	17.20(.02)
	17.25	17.18(.04)	17.29(.03)		19.05		16.85(.02)
	17.53	17.11(.05)	17.23(.03)				
	18.71	16.55(.02)	16.82(.03)				

TABLE II.   Composition of sharp fraction in blend (weight per cent)

Mixtures	PS1	PS2	PS3	PS4	PS5	PS6
1	49.84	49.66		.50		
2	72.93			27.07		
3	69.61		29.56		.83	
4	69.14		30.46			.40
5	62.84	26.93		8.68	1.56	
6	57.19	40.45			2.36	

TABLE III. Characteristics of sharp fractions

Sample	$\overline{M}_n$	$\overline{M}_w$	$\overline{M}_z$	$\overline{M}^u_{z+1}$
PS1	35(2)	36(2)	38(2)	40
PS2	108	115	122	130
PS3	153(3)	162(4)	177(7)	193
PS4	178	184	195(5)	207
PS5	391(14)	414(6)	460(39)	511
PS6	394(30)	508(7)	593(33)	692

Molecular mass averages of polystyrene sharp fractions used in blending experiments. Values enclosed in brackets are standard deviations in the mean estimated from the different methods.

TABLE IV. Molecular mass averages of mixtures

Mixtures	$\overline{M}_n$	$\overline{M}_w$	$\overline{M}_z$	$\overline{M}^{\ell}_{z+1}$	$\overline{M}^u_{z+1}$
1	59	76	103	116	123
2	45	76	141	180	191
3	46	76	144	206	226
4	46	76	143	210	235
5	48	78	145	237	258
6	50	77	142	254	279

Sharp fractions of polystyrene are available which are most unlikely to vary in microstructure, and which cover a wide range of molecular weights. Accordingly, sensitive effects of the MWD were here scrutinised for PS in absence of other complications.

Theory, rather than empiricism, can pin-point both which fundamental measurements and which technological properties are likely to be sensitive to the higher moments of the MWD. More important still, it can pin-point conditions for fundamental measurements which are most likely to bring out behaviour which correlates with practical performance. Not surprisingly, the condition of working with instruments which function near a Flory θ-point turns out to be crucial. This condition should equally cover variations in branching - as is already suggested by experimental and theoretical evidence (Ref. 16) - and no doubt variations in microstructure yet to be examined. We briefly summarise the arguments for focussing on near-theta conditions for a better approach to characterising polymers in respect of the relevant technological properties.

7.3 UNDISTURBED DIMENSIONS, BALANCE OF INTERACTIONS, AND SLOW RELAXATIONS

Fundamental characterisation depends on largely isolating the polymer coils from each other by means of an intruder: the solvent. At the theta point, the disturbing effect of the intruder is minimised in two respects: i) conformational coil dimensions and ii) interparticle interactions.

i) Coil dimensions

Flory's suggestion that a polymer chain in the bulk state has the same undisturbed dimensions as when it is isolated (infinite dilution) at the θ-temperature in a solvent has been thoroughly proved (Ref. 18). The θ-point is, of course, also the critical temperature T_c for a chain of infinite molecular weight M. At finite M, we find T_c a little below θ (for LCST systems) and at a concentration where chain-configurations are affected by some mutual overlapping of coils. The changes in temperature and concentration along the locus of critical points as a function of M (cf. the Shultz-Flory plot (19)) have opposing influence on chain dimensions, and we may assume (even for finite M) that in the vicinity of a critical point (ϕ_c, T_c), where spinodal and cloud points are most accurately measurable, we still have approximately the same coil configurations as in bulk.

ii) Balance of interactions

Besides, in this region near (ϕ_c, T_c), the segment/solvent interactions present in solutions are in a state of near-balance (equality) with the segment/segment interactions, which are, of course, the ones that control bulk properties of the polymer in the absence of intruding solvents. Correlations between spinodals or CPC's and technical properties might thus be expected. This is especially clear for properties which are sensitive to higher moments of the MWD.

Which technical bulk properties should be expected to correlate with spinodals and CPC's in solution? Surely we should look for those technical bulk properties near equilibrium, which are known already to depend on higher moments of the MWD. On the plane of fundamental theory we are directed immediately to the slow end of the relaxation spectrum, where indeed bulk behaviour has been successfully treated in terms of fundamental dilute-solution theories such as that of Rouse or Zimm (20). On the technological plane, the slow end of the spectrum concerns the final stages of all fabrication processes, when an article is left to relax towards equilibrium.

7.4 SPINODALS, CLOUD-POINTS, AND DIE-SWELL RATIOS

Thus technical properties governing dimensional stability, die-swell, surface gloss, etc. are dominated by slow relaxations to equilibrium, and therefore by higher moments of the MWD, just as equilibrium loci such as spinodals and CPC's in solution have been shown here to be controlled by higher moments also. Since we are dealing with similar (near-undisturbed) dimensions of the coils, and with similar segment/segment interactions also, parallelisms between superficially different situations should not surprise us. We briefly illustrate this for the steady-state compliance (Ref. 20) J_e^0 of a melt. No doubt because of difficulties in measuring higher moments, theories suggesting different patterns of moment-dependence sometimes exist side by side. An extended Rouse-Bueche theory by Ferry et al. (21) led to

$$J_e^0 \propto M_{z+1} \, M_z/M_w^2 = M_3/M_1^3 \equiv Q_1 \ (\text{say}) \tag{2}$$

while a theory of Mills (22) gave

$$J_e^0 \propto (M_z/M_w)^{3.7} = (M_2/M_1^2)^{3.7} \equiv Q_2 \ (\text{say}) \tag{3}$$

Thus the former theory predicts constant J_e^0 for all 3-equivalent distributions (here sharing moments M_1 and M_3, though M_2 is arbitrary), while the latter only requires 2-equivalence (i.e. sharing M_1 and M_2 ensures constant J_e^0). A preliminary rheogoniometric study by Irvine (12), based on the technique of using mixtures of sharp fractions, which was found fruitful above for spinodals and CPC's, gave ratios $J_e^0(\text{exp})/Q_1$ more nearly constant than $J_e^0(\text{exp})Q_2$, thus favouring the Rouse-Bueche-Ferry theory over Mills's. The blends were studied in solution (ca. 18% by weight) in decalin. Measurements of J_e^0 with more up-to-date equipment than available to Irvine should easily allow a firm discrimination.

The study of Vlachopolous and Alam (23) on melt fracture also suggests applications of the concept of r-equivalence. Their measurements of recoverable shear strain γ_r and die-swell ratio (d/D), measured at the critical shear stress σ_c, could be well explained by the Rouse-Bueche-Ferry theory. Thus 3-equivalent samples sharing constant M_1 and M_3, and hence constant Q_1, did have very similar die-swell ratios, as is to be expected, since γ_r and d/D should be proportional to $J_e^0 \cdot \sigma_c$.

7.5 A COMPARISON WITH GPC

Though the PICS instrument has important functions in the study of the phase behaviour of blends in bulk (Ref. 5), and can be used to study kinetics of crystallisation of polymers from solution (Ref. 24), we are here concerned with its potential for characterising polymers in solution. There is room for considerable differences in approach to characterisation. The proposal for characterising polymers in terms of spinodals and CPC's in theta solvents may be contrasted with the well-established and tested GPC technique. GPC accumulates

detailed information on the MWD by measurements on coils separated generally under conditions not near a theta point. The information is frequently too detailed to be used in technology without data reduction by means of a computer, usually in terms of summations yielding M_n and M_w. Calculation of M_z is only very approximate, and that of higher averages from GPC becomes progressively more hazardous.

GPC played a valuable part in characterising fundamentally the sharp fractions used in this study. Once they were mixed to produce the blends (Table II), however, PICS came into its own. Note that samples B-F would have MWD curves, determinable by GPC, which would look very different indeed, with numbers of peaks varying from two to four. Yet the spinodals of samples B-F were hardly distinguishable (Fig. 7) as predicted from their M_w and M_z, while their CPC's showed reasonable correlations with calculated M_{z+1}, which would be the average likely to be involved in die-swell.

Thus by working near theta-conditions, the data reduction (averaging with suitable weightings) can be performed directly and sensitively by a physical measurement (e.g CPC or spinodal), thus obviating the need for taking the polymer apart by fractionation in an instrument insensitive to high molecular weights, only to put it together again in a computer by an averaging process. Indeed one may hope that the balance of energetic and entropic effects which are measured as a spinodal or CPC in solution may correlate directly with other sensitive technical properties of bulk specimens beside those concerned with slow relaxations in the final stages of manufacture. But a systematic approach to improvements in characterisation is most likely to bear fruit in revealing correlations in a field, where the development of new instrumental techniques has to go hand in hand with that of physical and mathematical theories and of computing algorithms.

REFERENCES

1. M. Gordon, J. Goldsbrough, B.W. Ready and K.W. Derham, Brit. Pat. 1377478 (1975); U.S. Pat. 3807865 (1974).
2. K.W. Derham, J. Goldsbrough and M. Gordon, Pure and Appl. Chem. 38, 97-116 (1974).
3. M. Gordon, P. Irvine and J.W. Kennedy, J. Polym. Sci., Polymer Symposium 61, 199-220 (1977).
4. J.W. Kennedy, M. Gordon and G.A. Alvarez, Polimery, Warsaw, 10, 464-471 (1975).
5. R. Koningsveld, L.A. Kleintjens and M.H. Onclin, J. Macromol. Sci. Phys. B18, 363 (1980).
6. M. Gordon and P. Irvine, Macromolecules 13, 761 (1980).
7. Th.G. Scholte, J. Polym. Sci.A2 9, 1553 (1971); J. Polym. Sci. A2 8, 841 (1970).
8. H.A.C. Chermin, M. Gordon and R. Koningsveld, Macromolecules 2, 207 (1969).
9. R. Koningsveld and A.J. Staverman, J. Polym. Sci. A2 6, 349 (1968).
10. K.W. Derham, J. Goldsbrough, M. Gordon, R. Koningsveld and L.A. Kleintjens, Makromol. Chem. Suppl. 1, 401 (1975).
11. M. Gordon and B.W. Ready, U.S. Pat. 4131369 (1979); J.A. Torkington, L.A. Kleintjens, M. Gordon and B.W. Ready, Br. Polym. J. 10, 170-172 (1978); see also Ref. 5.
12. P. Irvine, Ph.D. Thesis, University of Essex, (1979).
13. P. Irvine and J.W. Kennedy, Macromolecules, submitted.
14. R. Koningsveld, W.H. Stockmayer, J.W. Kennedy and L.A. Kleintjens, Macromolecules 7, 73 (1974); L.A. Kleintjens, R. Koningsveld and W.H. Stockmayer, Br. Polym. J. 8, 29 (1976).
15. P. Irvine and M. Gordon, Proc. Roy. Soc. Lond. A. 375, 397-408 (1981).
16. L.A.L. Kleintjens, Ph.D. Thesis, University of Essex, (1979); L.A. Kleintjens, R. Koningsveld and M. Gordon, Macromolecules (in press); K.W. Derham and M. Gordon, Proceedings of Polymerphysik, Ch. Ruscher (Ed.), Phys. Ges.DDR, Berlin (Symposium held in Leipzig, 11-14 Sept.), (1974).
17. K.W. Derham, Ph.D. Thesis, University of Essex (1975).
18. P.J. Flory, Faraday Disc., Roy. Chem. Soc. 68, 14 (1979).
19. A.R. Shultz and P.J. Flory, J. Am. Chem. Soc. 74, 4760 (1952).
20. See J.D. Ferry, Viscoelastic Properties of Polymers 2nd Ed., Wiley, N.Y. (1970).
21. J.D. Ferry, M.L. Williams and D.M. Stern, J. Chem. Phys. 56, 987 (1954).
22. N.J. Mills, Eur. Polym. J. 5, 675 (1978).
23. J. Vlachopoulos and M. Alam, Polym. Eng. Sci. 12, 309 (1972).
24. D.M. Koenhen, C.A. Smolders and M. Gordon, J. Polym. Sci. Polymer Symposium 61, 93 (1977).